

Beyond Intra-modality: A Survey of Heterogeneous Person Re-identification

Zheng Wang, Zhixiang Wang, Yinqiang Zheng, Yang Wu, and Shin'ichi Satoh

Abstract—An efficient and effective person re-identification (ReID) system alleviates investigators' painful and boring video watching and accelerates the progress of the video investigation. Recently, with the explosive requirements of practical applications, a lot of research efforts have been dedicated to heterogeneous person re-identification (He-ReID). In this paper, beyond intra-modality, we start to review state-of-the-art He-ReID methods comprehensively concerning the challenges from inter-modality discrepancies. From the dimension of application scenario, we classify related methods into four categories – low-resolution, infrared, sketch, and text.

We begin with a diagram of person re-identification, then make a comparison between the general Homogeneous ReID (Ho-ReID) and He-ReID tasks. Then, we describe and compare available existing datasets for performing evaluations, and survey the models that have been widely employed in He-ReID. We also summarize and compare the representative approaches from two dimensions, *i.e.*, the application scenario, and the learning pipeline. Finally, we discuss some future research directions.

Index Terms—Person Re-identification, Heterogeneous, Cross-modality, Modality Discrepancy, Deep Learning

I. INTRODUCTION

In modern cities, important streets, public places, and critical areas have widely equipped video surveillance systems. In daily investigation and anti-terrorism events [1], investigators are used to exploit camera videos to re-identify persons, generate trajectories across camera views, and predict their behaviors. More importantly, when a big criminal case happens, video investigation is almost the most crucial means to find clues [2]. The impressive “2005 London subway bombings” and “2013 Boston marathon bombings” are uncovered with the help of surveillance videos [3]. Person re-identification (ReID) is now a valuable and hot topic in computer vision and machine learning communities [4], [5], [6], [7], [8], [9], [10], [11], [12], [13], [14], [15], [16], [17], which aims to retrieve the same person across non-overlapping cameras. An efficient and effective person re-identification (ReID) system alleviates investigators' painful and boring video watching and accelerates the progress of the video investigation. General ReID technologies have obtained very high accuracy on public datasets in recent years due to the dramatic research

Z. Wang, Y. Zheng and S. Satoh are with the Digital Content and Media Sciences Research Division, National Institute of Informatics, 2-1-2 Hitotsubashi, Chiyoda-ku, Tokyo 101-8430, Japan. (e-mail: wangz@nii.ac.jp; yqzheng@nii.ac.jp; satoh@nii.ac.jp).

Z. Wang (Co-first Author) is with the Department of Computer Science and Information Engineering, National Taiwan University, Taipei 106, Taiwan. (e-mail: wangzx1994@gmail.com).

Y. Wu is with the Computer Vision Lab, Kyoto University, Yoshida Honmachi, Sakyo-ku, Kyoto 606-8501, Japan. (e-mail: wuyang0321@gmail.com).

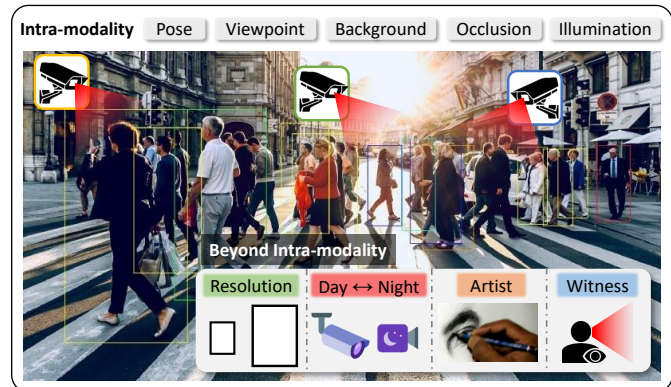


Figure 1. **Beyond Intra-modality.** Heterogeneous person re-identification encounters additional modality discrepancy, coming from the real application scenarios.

progress [18], [19], [20], [15], [16], for example, 94.4% accuracy (rank 1) on the Market-1501 [21] dataset and 97.8% on the CUHK03 [8] dataset, which outperform the ability of human [22]. However, the general ReID research has only been tested in the desired domain, which assumes that all person images are captured in the daytime with the visible spectrum and these images have sufficient pixels to represent a person. We define this type of person retrieval task as Homogeneous Person Re-identification (**Ho-ReID**).

In real applications, however, it is impractical to assume only working on such a desired domain, which only faces the challenges of intra-modality discrepancy, such as pose and viewpoint changes [23], [24], [25], [26], [27], [28], background and illumination variations [29], [30], [19], [31], [32], and occlusions [33], [34], [35]. For example, when a criminal case happens, the investigators likely have to check person images in low-resolution (LR), or captured by infrared (IR) cameras when the illumination condition is not sufficient. Moreover, witnesses' descriptions (in terms of text) and sketches drawn by artists shall also be used as the cues for finding a specific person from visual surveillance data. These scenarios should address new challenges beyond the intra-modality discrepancy investigated in Ho-ReID (Figure 1).

Therefore, as shown in Figure 2, more efforts should be made on matching persons' data across different domains/modalities, bridging the gap between different camera specifications and settings (*e.g.*, Low-resolution *vs.* High-resolution data), different sensory devices (*e.g.*, Infrared *vs.* Visual light devices), and reproduction of human memory and direct recording by a camera (*e.g.*, Sketches/Text Description



Figure 2. **Scope of heterogeneous person re-identification studied in this survey.** There are gaps between the desired domain (daytime, visible spectrum, and high-resolution) and other domains, including Low-Resolution (LR), Infrared (IR), Sketch images, and Text description. General homogeneous ReID (Ho-ReID) has so far only focused on the challenges within the desired domain, while He-ReID needs to handle extra challenges cross the desired and other collaborative domains.

vs. Digital images). We call this matching as Heterogeneous Person Re-identification. In most cases, He-ReID involves querying a gallery consisting of high-resolution visible light person images using a probe from another domain/modality.

Encouragingly, in the past a few years, we have already seen quite a number of remarkable signs of progress on He-ReID (including our contributions), which are primarily assisted by a growing variety of He-ReID benchmark datasets allowing direct comparison of different methodologies. *While general Ho-ReID attracts too much attention in the research community, causing very intense competition and homogeneous tendency of research, we feel that it is the right time to call for more attention and research efforts to the important and still largely unexplored area of He-ReID by providing a quality survey for both brave pioneers and wondering newcomers.* This paper offers a comprehensive and up-to-date review of the diverse and growing array of He-ReID techniques.

What are the differences between this survey and former ones? On the basis of our knowledge, there are few reviews in the ReID field [7], [36], [12], [37], [38], [39]. [38] explored the person re-identification applications built on gait sequences rather than person images, which is a special and different focus. [7], [36], [12], [37] focus on the general Ho-ReID task. Vezzani *et al.* [7] made a multidimensional overview of Ho-ReID, including camera settings, sample datasets, body models, machine learning methods and application scenarios. Zheng *et al.* [12] described critical future directions and briefed some important yet under-developed issues in Ho-ReID. Gou *et al.* [37] conducted a systematic evaluation with different features, metrics, and datasets in Ho-ReID. These

methods well shape Ho-ReID and position existing works and current progress. However, they have no investigation on He-ReID and confine their knowledge to the intra-modality discrepancy. Leng *et al.* [39] started to involve some inter-modality challenges, but they provided a limited in-depth summary of current efforts or detail the problems present in He-ReID. This survey seeks to highlight the difference between He-ReID and Ho-ReID, to provide a comprehensive summary of current research on He-ReID, and to analyze related works from different perspectives and presented some new insights toward this area.

Goals of this survey. The goals of this survey lie in three aspects. (1) We want to present the idea of He-ReID and raise awareness of this issue. (2) We thoroughly review the literature on the He-ReID task. For researchers in other fields, this survey provides a panorama with which readers can quickly understand and step into the new area of He-ReID. (3) This survey also gives comprehensive guidance of future directions to the researchers in this field.

Contributions of this survey. To achieve these goals, the main contributions of this survey are three-fold: (1) Beyond intra-modality, we conduct a systematic review for Heterogeneous Person Re-identification, where the inter-modality discrepancy works as the main challenge. (2) We categorize related works into different modalities they operate across, provide an overview, and summary for the state-of-the-arts. As Figure 2 shows, we consider four cross-modality application scenarios: Low-resolution (LR), Infrared (IR), Sketch, and Text. (3) We analyze representative methods and identify future directions in this research field to share the vision and expand the horizons of He-ReID.

The following parts of this survey are organized as follows: Section II illustrates the basic idea and diagram of person re-identification, then gives an introduction of the scope of Ho-ReID and He-ReID. Section III makes a brief comparison between the Ho-ReID and He-ReID. Section IV introduces and organizes the available datasets for performance evaluation in each category. Section V summarizes and compares the representative approaches. Section VI closes by drawing overall conclusions and making recommendations for potential research directions which are worth pursuing.

II. PERSON RE-IDENTIFICATION

A. Person Re-identification Diagram

Figure 3 gives the diagram of the person re-identification system, including feature extraction part and descriptor matching part. For the gallery, feature extraction is firstly carried out, and robust feature vectors are extracted and stored in the database, which are to be used in the descriptor matching stage. When the system is input a probe person, the person's feature vector is automatically obtained by the feature extraction part. After that, the feature vector of the probe matches against the feature vectors in the database by distance metric or feature classification technologies.

For the general Ho-ReID task, both the probe and gallery are from the desired domain (daytime, visible spectrum, and high-resolution) images. While for the He-ReID task, the probe and

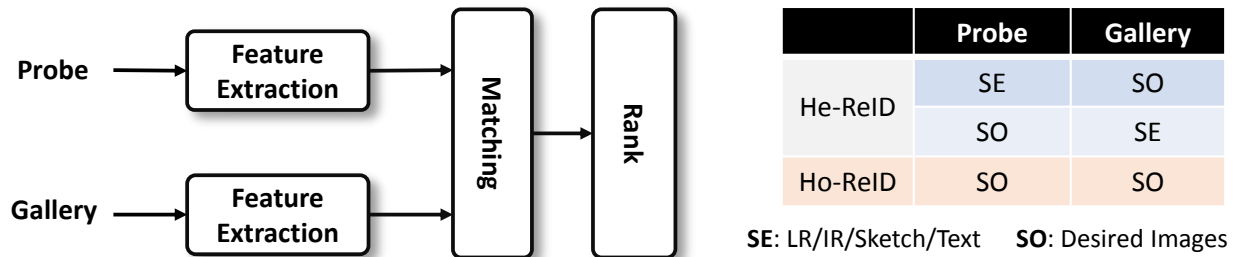


Figure 3. The person re-identification diagram.

gallery are from different sources. For instance, if the gallery consists of desired images, the probe will LR image, IR image, Sketch or Text.

B. Ho-ReID: Intra-modality

General Ho-ReID task only faces the challenges of person’s appearance changes, such as pose and viewpoint variations, occlusions and illumination differences. Persons’ images are captured in the desired domain with only the intra-modality discrepancy. Following the diagram of person re-identification, some researches tried to design robust and discriminative features [40], [41], [4], [6], [10], [11], [42], [43], [44], other researches attempted to learn effective distance metrics [45], [46], [47], [48], [49] or subspaces [50], [51], [52], [53], while currently most of the researches started to focus on deep learning models [8], [54], [55], [56], [57], [58], [59], [14], [15], [60], [61], [62], [63]. Some ReID surveys exist [7], [36], [12], [37]. For more details, the readers can refer these surveys.

C. He-ReID: Beyond Intra-modality

He-ReID task should face more challenges beyond the intra-modality discrepancy, such as HR-to-LR discrepancy, RGB-to-IR discrepancy, Photo-to-Sketch discrepancy, and Image-to-Text discrepancy. These extremely large discrepancies are generated from different modalities. Hence, approaches in the He-ReID field should pay more attention to remove the inter-modality discrepancy. Some cross-modality related surveys in other areas, *e.g.*, face recognition [64] and image retrieval [65], also raise the urgent requirements of addressing the inter-modality discrepancy and set an example to us.

Note that we don’t attribute the RGB-depth based ReID to our He-ReID task, although there are a couple of researches investigated this kind of task. For instance, Barbosa *et al.* [66] were the first to investigate the ReID problem through the data generated by RGB-depth sensors. Mogelmose *et al.* [67] proposed a joined classifier combining the features of RGB, depth, and thermal data. Munaro *et al.* [68] constructed the BIWI RGBD-ID dataset, created 3D models, and performed re-identification by matching body shapes. Haque *et al.* [69] leveraged unique 4D spatio-temporal signatures and proposed a re-identification model based on a combination of CNN and RNN. Wu *et al.* [70] used depth voxel covariance descriptor and proposed a kind of Eigen-depth feature to describe pedestrian body shape. In practical surveillance situation, we will not use a depth image of a person to retrieval in an

RGB image gallery. Since RGB-depth camera always works to generate four-channel (RGBD) images simultaneously, rather than three-channel RGB images and one-channel depth images separately. The depth channel works as a complement for the RGB channels.

III. HETEROGENEOUS REID vs. HOMOGENEOUS REID

We make a brief comparison between the Ho-ReID and He-ReID, as Table I shows. For the re-identification media type, general Ho-ReID only exploits the desired RGB images, while He-ReID takes additional LR/IR/Sketch images and Text description into account. For the participant, the Ho-ReID technology only employs the resources from machine intelligence, while He-ReID also brings the input from human, such as the sketch image drawn by a painter or text description of the suspect by the witness. Hence, *He-ReID is a more valuable task for practical video investigation applications.*

For the main challenge, Ho-ReID only needs to deal with the intra-modality discrepancy, such as viewpoint variations, image misaligned or occlusion and illumination changes, while He-ReID should mainly bridge the gaps deriving from both intra- and inter-modality discrepancies. Since additional inter-modality discrepancies introduced, which are larger than intra-modality discrepancies [71], He-ReID is more challenging than Ho-ReID. As intra-modality and inter-modality discrepancies are essentially different, the methods designed for Ho-ReID cannot be directly used in He-ReID. Currently, the performances of Ho-ReID methods are high, while the performances of He-ReID methods are low. Hence, *we should investigate how to eliminate the inter-modality discrepancy for the He-ReID task.*

Figure 4(a) makes a comparison of state-of-the-art performances of Ho-ReID and He-ReID tasks. The results are on the typical datasets, *i.e.*, the Market-1501 dataset [21] for Ho-ReID, the MLR-VIPER dataset [72] for He-ReID LR task, the SYSU-MM01 dataset [75] for He-ReID IR task, the Sketch Re-ID dataset [73] for He-ReID Sketch task, and the CUHK-PEDES dataset [76] for He-ReID Text task. We can find that all of the state-of-the-art performances of He-ReID tasks are still not so satisfied as that of the Ho-ReID task. He-ReID is a more challenging problem, compared with general Ho-ReID problem, since we need to fill the gap between the LR/IR/Sketch/Text domain and the desired image domain. However, compared with Ho-ReID, there are not so many publications related to He-ReID (Figure 4(b) shows). Considering the realistic value and research significance, we

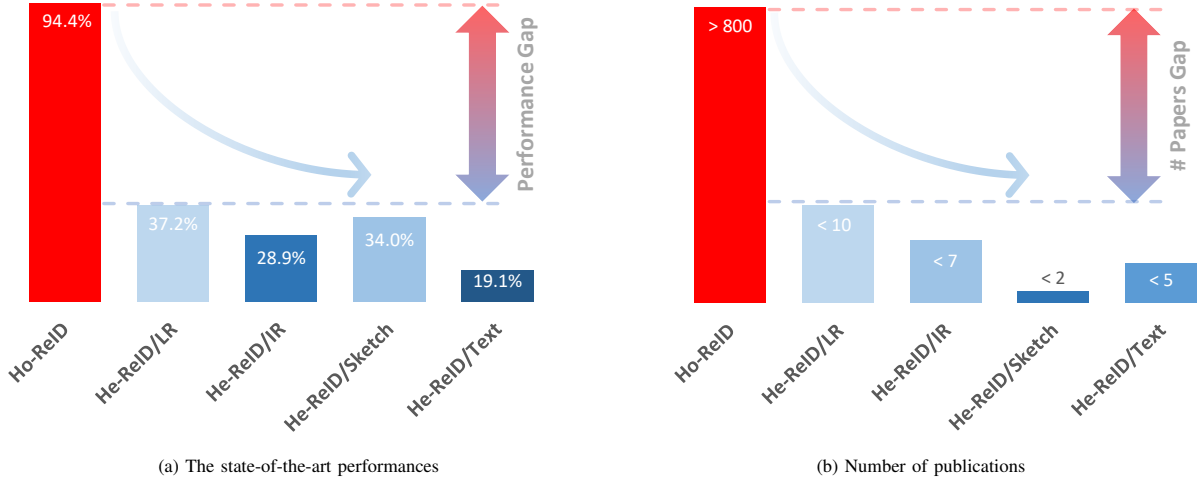


Figure 4. **Comparison between Ho-ReID and He-ReID.** (a) The state-of-the-art performances. The compared methods are respectively AlignedReID [22] for the Ho-ReID task, SING [72] for the He-ReID LR task, D²RL [71] for the He-ReID IR task, CDAFL [73] for the He-ReID Sketch task and CNN-LSTM [74] for the He-ReID Text task. There is a big performance gap between the LR/IR/Sketch/Text domain and the desired image domain. Note that we use the CMC-1 value to represent the performance. Since we would like to show the big performance gap between Ho-ReID and He-ReID tasks, so we do not make a comparison of different methods within a task. (b) Number of publications. Compared with Ho-ReID, there are not so many publications related to He-ReID.

Table I
COMPARISON BETWEEN HO-REID AND HE-REID. ‘#PUBLICATIONS’ REPRESENTS FOR THE NUMBER OF PUBLICATIONS RELATED TO HO-REID OR HE-REID.

	Ho-ReID	He-ReID
Media Type	Desired image	+ LR/IR/Sketch/Text
Participant	Machine	Human & Machine
Main Challenge	Intra-modality	Intra- + Inter-modality
Performance	High	Low
#Publications	>800	<50

feel that it is the right time to call for more attention and research efforts to the area of He-ReID.

IV. AVAILABLE DATASETS AND EVALUATION METRICS

In this section, we make a survey of available datasets and give an introduction of evaluation metrics. For the datasets, we first show some typical Ho-ReID datasets, then list most of the He-ReID datasets.

A. Ho-ReID Datasets

The **VIPeR** [77] dataset is constructed by the images of 632 persons in the outdoor environment. It contains 1,264 images, in which each person has two images captured from two different views. Generally, the dataset is often randomly split into two subsets, *i.e.*, one subset of image pairs is for training and the other one is for testing. The **3DPES** [78] dataset is also constructed in the outdoor environment. All images are captured from eight non-overlapping cameras. In total, the dataset includes 1,011 images from 192 individuals, in which each person has 2 to 26 images. The **i-LIDS** [79]

dataset is constructed by multiple different camera views. The dataset includes 476 person images captured from 119 persons, in which each person has 4 images on average. The **PRID 2011** [80] dataset is built from by two non-overlapping cameras. One camera captures images from 385 persons, and the other camera contains images from 749 persons. 200 of those persons appear in both camera views. The **PRID 450S** [81] dataset is built under the same environment as the PRID 2011 dataset, in which images are captured over two non-overlapping cameras. It includes 900 images from 450 persons, *i.e.*, each person has two images respectively from two different views. The **CUHK03** [8] dataset is built in the CUHK campus. Two non-overlapping cameras are exploited to capture person images. The whole dataset includes 14,096 images from 1,467 persons, in which each person has 4.8 images in each camera on average. The dataset presents data in two means, *i.e.*, ‘labeled’ and ‘detected’, where researchers can conduct experiments on both means. The **Market-1501** [21] dataset is currently one of the largest benchmark dataset for Ho-ReID. The person images are captured from six cameras. Some examples are shown in Figure 5(a). Totally, the dataset includes 32,668 images from 1,501 persons. The **DukeMTMC-reID** [13] dataset is another large-scale dataset, which is built by eight cameras in Duke University. Images of 1,812 persons are captured. Among those individuals, 1,404 persons appear in more than two cameras, and 408 persons act as distractor ones.

B. He-ReID Datasets

We list available datasets for He-ReID in Table II, including the application scenario, the total number of cameras, identities, and samples. To make a comparison, we also list some typical Ho-ReID datasets. In particular, we take notice of the data construction type. From this view, we can find that some datasets are constructed by simulated images.

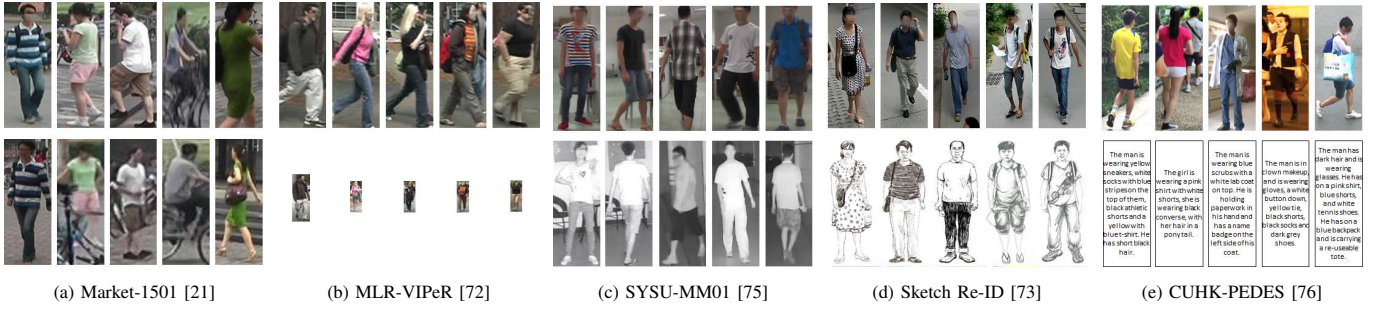


Figure 5. **Examples of available Datasets.** From left to right, the datasets are representative ones, respectively Ho-ReID dataset (Market-1501), He-ReID LR dataset (MLR-ViPeR), He-ReID IR dataset (SYSU-MM01), He-ReID Sketch dataset (Sketch Re-ID) and He-ReID Text dataset (CUHK-PEDES).

1) *He-ReID LR datasets:* The **CAVIAR** [82] is built in a shopping mall. Images of 72 persons are captured by two different camera views. The resolution of images captured from one camera is much lower than that in the other one. In general experimental setting, 22 persons are not included, since those are only captured in the high-resolution camera. After removing those 22 persons, the dataset includes 1,000 images from 50 persons, in which each person has ten relative high-resolution images and 10 low-resolution images. The **LR-ViPeR** and **LR-3DPES** [83] datasets are respectively simulated from the **ViPeR** and **3DPES** datasets. For both of the datasets, half of the images are replaced with down-sampled low-resolution images whose size is $1/4$ of the original image size. The **LR-i-LIDS** and **LR-PRID** [84] datasets are respectively simulated from **i-LIDS** and **PRID 2011** datasets. For both of the datasets, half of the images are replaced with down-sampled low-resolution images as well. For each person, the original image is set into the high-resolution set, while another image is down-sampled and smoothed to generate a low-resolution set. The sampling rate is $1/8$. The **SALR-ViPeR** and **SALR-PRID** [85] datasets are respectively simulated from **ViPeR** and **PRID 450S** datasets. For both of the datasets, images from one camera are set as the HR probe set, whose resolution remains unchanged. While images from the other camera, which are down-sampled randomly to different scales, are set as the LR gallery set. The scale ratio ranges from $1/10$ to $1/4$. The **MLR-ViPeR**, **MLR-CUHK03** and **MLR-SYSU** [72] datasets are respectively simulated from **ViPeR**, **CUHK03**, and **SYSU** datasets. **SYSU** [87] has totally 24,446 images of 502 people captured by two cameras. Three images per person per camera are selected and created LR images. Images from one camera view are down-sampled by a ratio randomly picked from $\{1/2, 1/3, 1/4\}$ whilst images of another view are remaining the same. Figure 5(b) shows some samples for **MLR-ViPeR**.

2) *He-ReID IR datasets:* The **SYSU-MM01** [75] dataset is built upon six cameras, *i.e.*, four RGB cameras and two infrared cameras. Among the six cameras, some are in the indoor environment, and the others are in the outdoor environment. Note that all the IR cameras are the active IR cameras. Images are captured from 491 persons. For the training, 22,258 RGB images and 11,909 infrared images are used, which are generated from 395 persons. For the testing, 3,803 infrared images for query and 301 randomly selected

RGB images for the gallery are used, which are captured from 96 persons. Some examples are shown in Figure 5(c). The **RegDB** [86] dataset is another He-ReID IR dataset. The difference is that the IR camera is a passive one. The dataset is built on two cameras, *i.e.*, one RGB camera and one infrared camera. Images are captured from 412 persons, in which each person has ten different RGB images and ten different infrared images.

3) *He-ReID Sketch dataset:* The **Sketch Re-ID** [73] dataset is the only one He-ReID Sketch dataset for person re-identification. Some examples are shown in Figure 5(d). Pang *et al.* [73] invited five artists to draw persons' sketches for 200 persons, in which each person has two photos, and then constructed a small-scale sketch dataset, in which each person has one sketch. For the training samples of 150 persons are used, while the remaining samples of 50 persons are used for the testing.

4) *He-ReID Text dataset:* The **CUHK-PEDES** [76] dataset is the only one He-ReID Text dataset for person re-identification. Some examples are shown in Figure 5(e). Li *et al.* [76] collected 40,206 images of 13,003 persons from the other datasets, and then described each image with two sentences. For the training, 34,054 images and 68,108 sentences of 11,003 persons are used, while 3,078 images of 1,000 persons and 3,074 images of 1,000 persons are respectively used for the validation and the testing.

5) *Summary:* For He-ReID datasets, we make the following summaries:

- Although many He-ReID LR datasets were constructed, most of them are simulated *w.r.t.* from general Ho-ReID datasets.
- Only two He-ReID IR datasets exist. **SYSU-MM01** [75] is an active IR dataset, while **RegDB** [75] is passive one. Only one He-ReID Sketch dataset and one He-ReID Text dataset are constructed.
- Compared with Ho-ReID, there is still a lot of room to construct more available datasets. For He-ReID LR, it requires to construct practical datasets instead of the simulated ones. For the other three kinds of application scenarios, datasets under different conditions/styles or with larger scales should be constructed.

Table II

RELEASED AND FREELY AVAILABLE DATASETS FOR HO-REID AND HE-REID. THE NOTATION ‘DESIRED’ INDICATES THAT THE DATASET IS CONSTRUCTED BY DESIRED RGB IMAGES. THE ‘SIMULATED’ INDICATES THAT THE DATASET IS CONSTRUCTED BY SIMULATED IMAGES. ‘APPL.’ INDICATES THE APPLICATION SCENARIO THE DATASET RELATED TO. ‘#CAMERA’, ‘#ID’ AND ‘#SAMPLE’ RESPECTIVELY REPRESENT FOR THE TOTAL NUMBER OF CAMERAS, IDENTITIES AND SAMPLES.

Dataset	Appl.	Type	#Camera	#ID	#Sample
VIPeR [77]	Desired	Real	2	632	1,264
3DPES [78]	Desired	Real	8	192	1,011
i-LIDS [79]	Desired	Real	2	119	476
PRID 2011 [80]	Desired	Real	2	934	1,134
PRID 450S [81]	Desired	Real	2	450	900
CUHK03 [8]	Desired	Real	2	1,360	13,164
Market-1501 [21]	Desired	Real	6	1,501	32,668
DukeMTMC-reID [13]	Desired	Real	8	1,404	36,411
1 CAVIAR [82]	LR	Real	2	50	1,000
2 LR-VIPeR [83]	LR	Simulated	2	632	1,264
3 LR-3DPES [83]	LR	Simulated	8	192	1,011
4 LR-i-LIDS [84]	LR	Simulated	2	119	238
5 LR-PRID [84]	LR	Simulated	2	100	200
6 SALR-VIPeR [85]	LR	Simulated	2	632	1,264
7 SALR-PRID [85]	LR	Simulated	2	450	900
8 MLR-VIPeR [72]	LR	Simulated	2	632	1,264
9 MLR-SYSU [72]	LR	Simulated	2	502	3,012
10 MLR-CUHK03 [72]	LR	Simulated	2	1,467	14,000
11 SYSU-MM01 [75]	IR	Real	6	491	38,271
12 RegDB [86]	IR	Real	2	412	8,240
13 Sketch Re-ID [73]	Sketch	Real	2	200	400
14 CUHK-PEDES [76]	Text	Real	–	13,003	80,412

C. Evaluation Metrics

Evaluation metrics are the same for the Ho-ReID and He-ReID tasks. When evaluating He-ReID methods, we often choose the Cumulative Matching Characteristics (CMC) [88] curve and the mean average precision (mAP) [21] as the evaluation metrics.

In practice, when only one ground truth exists in the gallery, or we are caring about the true matches ranking in top positions of the returning list, CMC curve is an acceptable selection. On the other hand, if multiple true matches exist in the gallery and we would like to retrieval all the results, mAP is a good selection. Since mAP cares more about the ability of

retrieval recall, while CMC does not. Hence, CMC and mAP are always used together for He-ReID tasks.

V. HE-REID METHODS

In this section, we make a survey of He-ReID methods from two dimensions. From the dimension of application scenario, we classify all related methods into four kinds of He-ReID application scenarios, which are the He-ReID LR, He-ReID IR, He-ReID Sketch, and He-ReID Text scenarios respectively. From the dimension of learning pipeline, we categorize typical methods into three types, which are (1) separated representation learning and metric learning, (2) shared representation learning, and (3) modality unifying and shared representation learning.

A. From the Dimension of Application Scenario

1) *He-ReID LR*: Commonly, the resolution of surveillance person image varies a lot, due to variations in the person-camera distance and camera deployment settings [90]. He-ReID LR application scenario attempts to compare images with different resolutions, where one is the normal resolution, and the other is low-resolution.

Jing *et al.* [84] was the first to investigate He-ReID task in the LR application scenario. They designed a semi-coupled low-rank discriminant dictionary learning method, constructing a relationship mapping from the features of normal person images to that of LR person images. Li *et al.* [83] proposed a joint multi-scale learning framework by learning metrics on feature domains of two different image scales simultaneously. Wang *et al.* [85] changed the problem to be low-resolution with different scales. They observed that scale-distance functions could be classified, and then learned a surface in function space to separate functions to identify persons. Jiao *et al.* [72] developed a super-resolution and identity joint learning method to improve the He-ReID LR performance. Similar to [84], Li *et al.* [89] designed a semi-coupled projective dictionary learning model to bridge the gap across different resolutions. Chen *et al.* [91] combined a resolution adaptation network and a re-identification network together to solve He-ReID LR problem. Ma *et al.* [97] extended their focus to video-based ReID matching problem (low-resolution and high-resolution videos) with different scales and designed a set-to-set distance learning method with semi-coupled mapping. Wang *et al.* [90] first cascaded multiple SR-GANs in series to promote the ability of scale-adaptive super-resolution, then plugged-in a re-identification network to enhance the ability of person representation. Mao *et al.* [92] jointly trained a Foreground-Focus Super-Resolution module and a Resolution-Invariant Feature Extractor, and then obtained a strong resolution invariant representation.

2) *He-ReID IR*: As we know, the visible cameras are not able to capture clear and valid appearance information under poor illumination environments (*e.g.* during the nighttime), which limits the applicability of person re-identification in practical surveillance applications. Therefore, He-ReID IR application scenario provides a good supplement for nighttime surveillance applications [94].

Table III

REPRESENTATIVE METHODS EMPLOYED IN HE-REID. THE NOTATION ‘CONF.’ INDICATES THE CONFERENCE THAT THE CORRESPONDING PAPER WAS PUBLISHED IN. ‘APPL.’ INDICATES THE APPLICATION SCENARIO THE PAPER STUDIES IN. ‘SEP.RL+ML’, ‘SHARED RL’ AND ‘MU+SHAREDRL’ RESPECTIVELY REPRESENT FOR THE PIPELINES THE CORRESPONDING UTILIZED. ‘SEP.RL+ML’ STANDS FOR SEPARATED REPRESENTATION LEARNING AND METRIC LEARNING (PIPELINE (A)). ‘SHARED RL’ STANDS FOR SHARED REPRESENTATION LEARNING (PIPELINE (B)). ‘MU+SHAREDRL’ STANDS FOR MODALITY UNIFYING AND SHARED REPRESENTATION LEARNING (PIPELINE (C)). ‘DATASETS’ INDICATES THE EVALUATED DATASETS IN THE PAPER, WHERE THE NUMBER DENOTES FOR THE CERTAIN DATASET IN TABLE II.

Reference	Appl.	Year	Conf.	Method	Datasets	Sep.RL+ML	Shared RL	MU+SharedRL
Li <i>et al.</i> [83]	LR	2015	ICCV	Metric Learning	1 2 3	✓		
Jing <i>et al.</i> [84]	LR	2015	CVPR	Dictionary Learning	2 4 5		✓	
Wang <i>et al.</i> [85]	LR	2016	IJCAI	Subspace Learning	1 6 7		✓	
Jiao <i>et al.</i> [72]	LR	2018	AAAI	Super Resolution	1 8 9 10			✓
Li <i>et al.</i> [89]	LR	2018	AAAI	Dictionary Learning	2 4		✓	
Wang <i>et al.</i> [90]	LR	2018	IJCAI	Super Resolution	1 6 7			✓
Chen <i>et al.</i> [91]	LR	2019	AAAI	Feature Learning	1 8 10		✓	
Mao <i>et al.</i> [92]	LR	2019	IJCAI	Super Resolution	1 8 10			✓
Wu <i>et al.</i> [75]	IR	2017	ICCV	Deep Zero-Padding	11		✓	
Ye <i>et al.</i> [93]	IR	2018	AAAI	Metric Learning	12	✓		
Ye <i>et al.</i> [94]	IR	2018	IJCAI	Feature Learning	11 12		✓	
Dai <i>et al.</i> [95]	IR	2018	IJCAI	Feature Embedding	11		✓	
Wang <i>et al.</i> [71]	IR	2019	CVPR	Image Generation	11 12			✓
Pang <i>et al.</i> [73]	Sketch	2018	ACM MM	Feature Learning	13		✓	
Li <i>et al.</i> [76]	Text	2017	CVPR	Affinity Learning	14		✓	
Li <i>et al.</i> [74]	Text	2017	ICCV	Feature Learning	14		✓	
Chen <i>et al.</i> [96]	Text	2018	ECCV	Association Learning	14		✓	

Wu *et al.* [75] was the first to investigate He-ReID task in the IR application scenario. They made a discussion and evaluation with three types of network structures for this task, which are respectively one-stream, two-stream and asymmetric *FC* layer structures. They also proposed a deep zero-padding module to improve the one-stream network, making the implicit network structure more suitable. Ye *et al.* [93] jointly optimized the modality-specific and modality-shared metrics and designed a hierarchical cross-modality matching model. Ye *et al.* [94] also attempted to learn discriminative features with an end-to-end framework. They proposed a dual-path network by exploiting a bi-directional dual-constrained top-ranking loss function. Dai *et al.* [95] proposed to learn discriminative common representations. The network consists of a generator for learning image representations and a discriminator, which tries to discriminate the modalities of RGB and IR images. Kang *et al.* [98] simplified the CNN structure by setting visible and infrared images as the common single

input. Wang *et al.* [71] presented a new framework, taking advantage of CycleGAN to reduce modality discrepancy from image-level and advantage of sophisticated Ho-ReID models to reduce appearance discrepancy from feature-level.

3) *He-ReID Sketch*: When someone reports a criminal case while the suspect was not identified by the surveillance camera, we call for an algorithm to automatically pick out the potential suspects according to a sketch by an artist’s drawing. Consequently, investigators will be able to narrow down and hence expedite their search [73].

Pang *et al.* [73] was the first and only one to investigate He-ReID task in the Sketch application scenario. They not only raised a dataset, but also proposed to learn identity features and domain-invariant features by exploiting a cross-domain adversarial feature learning framework.

4) *He-ReID Text*: As He-ReID task in the Sketch application scenario, searching a person with free-form natural language description (sentences) can be widely applied in

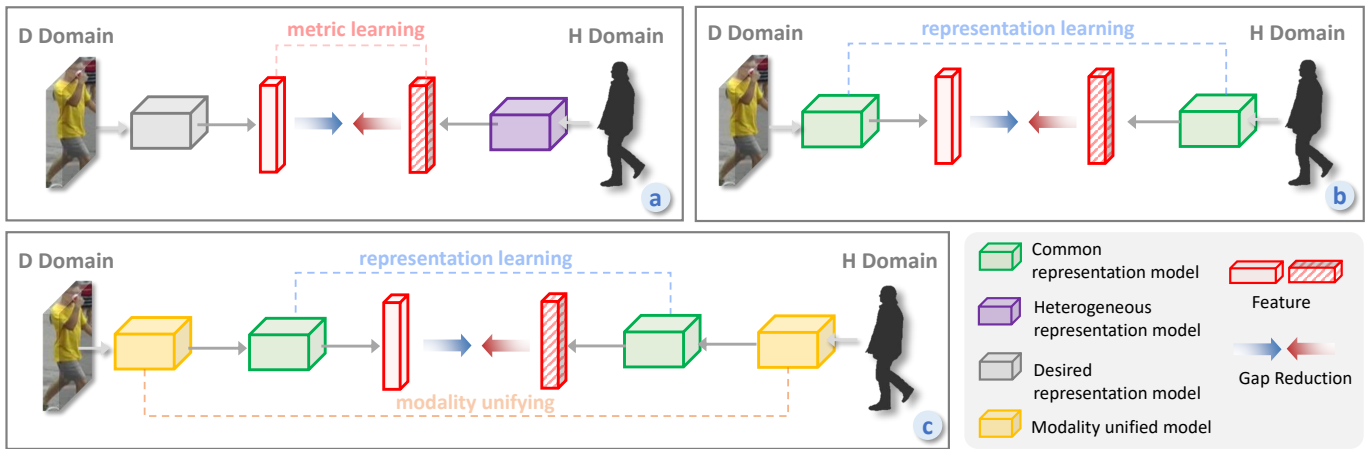


Figure 6. **Summary of three pipelines.** (a) just utilizes some metric learning method to learn how to match representations from separate representation models; (b) focuses on learning the common representation of different modalities; (c) pays attention to generating the modality-unified samples and then learning the common representation. In the figure, ‘D Domain’ stands for the samples from the desired domain. ‘H Domain’ stands for the samples from the heterogeneous domain.

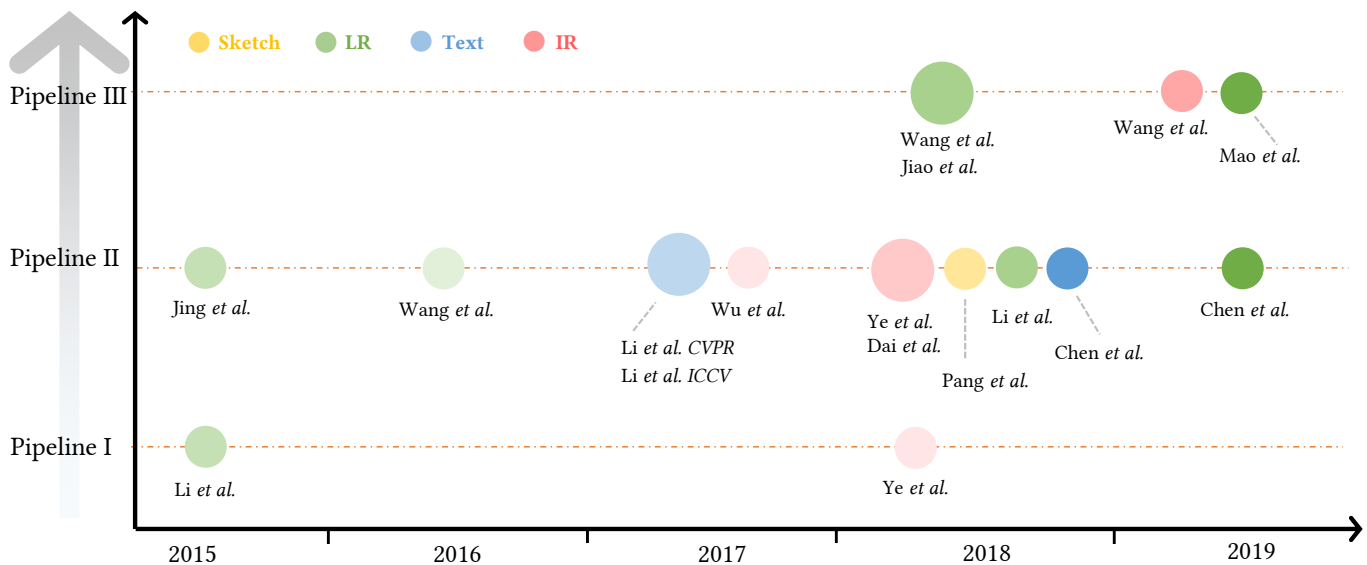


Figure 7. **Milestones of He-ReID.** We show some milestone methods according to its publication year (horizontal axis) and its category (vertical axis). The green, pink, yellow and blue circles stand for the He-ReID LR, IR, Sketch, and Text methods, respectively. The color brightness of the circle indicates the performance of the corresponding method, where darker the color is, the better performance it gets. The area of the circle indicates the number of publications, where larger the area is, more the quantity is. Pipeline (a) stands for the category of separated representation learning and metric learning. Pipeline (b) stands for the category of shared representation learning. Pipeline (c) stands for the category of modality unifying and shared representation learning.

video surveillance and activity analysis systems. It is in urgent need to pick up potential criminal suspects from large-scale videos [76].

In the early years, some researches started to investigate the re-identification with attribute-based queries [2], [99], [100], [101]. He-ReID Text application scenario denotes a situation that the queries are natural language descriptions. Li et al. [76] evaluated and compared a wide range of possible models, and proposed an RNN with Gated Neural Attention mechanism. Li et al. [74] designed an identity-aware framework for this problem. The two-stage framework firstly learned to embed cross-modal features, and then refined the matching results with a co-attention mechanism. Chen et al. [96] attempted to build global and local image-language associations. They

enforced semantic consistencies between local visual and linguistic features. Chen et al. [102] proposed a patch-word matching model and designed an adaptive threshold mechanism into the model.

5) *Summary:* For He-ReID methods, we make the following summaries:

- *Most of the methods selected a deep learning framework.* It is probably because all the heterogeneous application scenarios are raised in recent years, and the deep learning methods are in the high-speed development period. The deep learning methods have their superior on shared feature learning and image generating.
- *Different methods focused on different stages to fill the gaps between the desired domain and other heteroge-*

neous domains. Some of them [83], [75] try to learn a metric to fill the gap of features of different modalities. Some of them [84], [93], [91] attempt to learn shared features. Some of them [71], [90], [92] unify the modality in the data level. In Section V-B, we will make an analysis and discussion for the methods.

- *The existing researches in each application scenario still have much limitations.* For the He-ReID LR application scenario, recent researches are mainly evaluated on the simulated datasets. For the He-ReID Sketch application scenario, only one research touched this direction, due to the hardness of building a benchmark. The researches on He-ReID Text application scenario are also not so many, because only one dataset is constructed.

B. From the Dimension of Learning Pipeline

Representative methods employed in He-ReID are listed in Table III. For easy comparison, we list most of the valuable information of the works, including the published paper, year, conference, application scenario, method, and pipelines. We can find that all of the representative works are published in the recent five years. It means that He-ReID is a relatively new research topic. Among all the application scenarios, He-ReID Sketch and Text are less investigated. As described in the sections above, we consider that if more datasets are available, more works could be conducted and published. Particularly, He-ReID is a cross-modality task. To address the inter-modality discrepancy, in our opinion, representative methods can be categorized into three kinds of learning pipelines.

Figure 6 shows the diagrams of the pipelines. Pipeline (a) employs the metric learning method to learn how to match the features from separate representation learning models, and the representation learning models are trained separately with single modality data samples. Pipeline (b) focuses on learning shared feature models of different modalities, and training data come from both modalities. Pipeline (c) pays attention to generating the unified-modality samples, for example, using a super-resolution method to generate high-resolution images from low-resolution images, or using some image generation method to generate infrared images from RGB images and RGB images from infrared images.

We also analyze all listed representative methods and contribute the methods to these three pipelines (Figure 7). It also shows in Table III. For each kind of application scenario, from top to bottom, the methods become more effective. We can find that pipeline (c) performs better than pipeline (b), and better than pipeline (a). Hence, unifying the modality of samples is the most effective way to fill the modality gap. For the He-ReID LR application scenario, the super-resolution methods can be used, such as [90], [92]. Thanks to the developments of GAN, unifying the modalities is considerable as [71].

VI. CONCLUSION AND FUTURE DIRECTIONS

This paper attempted to provide an overview of recent developments of Heterogeneous Person Re-identification (He-ReID). It covers most of the literature on He-ReID. We summarized the widely employed methods, released datasets,

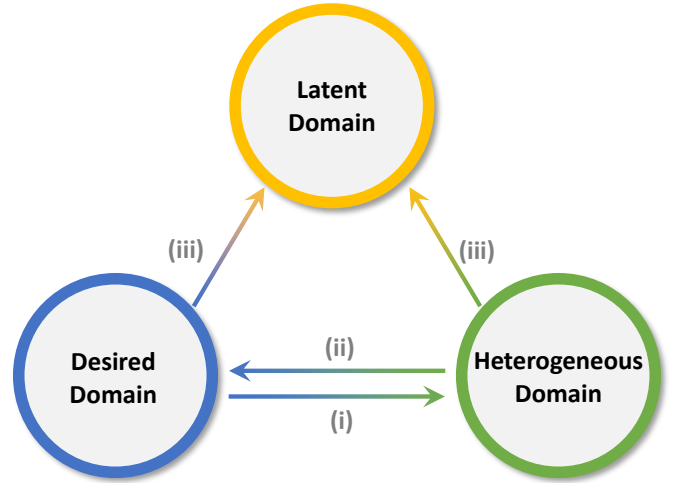


Figure 8. **Three kinds of domain transfer.** To unify the modality, we can transfer (i) from heterogeneous domain to desired domain, (ii) from desired domain to heterogeneous domain, and (iii) from both desired and heterogeneous domains to a latent domain.

and compared the existing methods. We believe that He-ReID will continue to be an active and promising research area with broad potential applications. Many issues in He-ReID, however, are still open.

Dataset Construction. For He-ReID LR application scenario, the researchers can only get simulated datasets. For the other types of applications, although the researchers can achieve practical datasets, the choice is limited. In addition, large scale He-ReID datasets are also required. It is somehow urgent for us to built new datasets, and push forward this research area.

Taking Advantage of Ho-ReID Datasets and Methods. There are sufficient datasets and methods in Ho-ReID field. It is easy to address the intra-modality discrepancy in the desired domain. Obviously, the feature space of the desired domain will be well-constructed. Since the desired domain samples are not enough, it is hard to build a perfect heterogeneous domain. However, it is reasonable to project the He-ReID samples into the desired domain.

Human Interaction and Crowdsourcing. For He-ReID Sketch and Text application scenarios, human intelligence joins into the process of re-identification. Human intelligence is sometimes subjective and incomplete. So we should consider how to mine and integrate useful information to help search the target in the surveillance system. On the hand, a lot of witnesses will provide their cues. Each person may have a different view so that the crowdsourcing cues may be diverse to each other. We should design a strategy to remove conflict and filter valuable information.

Investigation on Unifying the Modality. For He-ReID LR application scenario, some work [90], [92] attempted to use super-resolution methods to unify the modality, where they transfer the heterogeneous domain LR image to the desired domain. For He-ReID IR application scenario, with the help of CycleGAN, one work [71] not only transferred the image from heterogeneous (IR) domain to desired (RGB) domain but also transferred the image from desired domain

to heterogeneous domain. However, for the He-ReID Text and Sketch application scenarios, no work has investigated to unify the data modality. On the other hand, we can also investigate to unify the modality to a latent domain as Figure 8 shows, for example, a middle-level resolution for the He-ReID LR application scenario and a hyperspectral image for the He-ReID IR application scenario.

Integrating Multiple He-ReID Application Scenarios. For a practical system, it may require different kinds of inputs to search out the target. The He-ReID application scenarios can be equipped in different stages. If we can integrate different kinds of inputs, more valuable information could be used for retrieval, since different inputs have different attentions and views for the target. It would raise a novel multiple cross-domain research task.

REFERENCES

- [1] O. Camps, M. Gou, T. Hebble, S. Karanam, O. Lehmann, Y. Li, R. J. Radke, Z. Wu, and F. Xiong, "From the lab to the real world: Re-identification in an airport camera network," *IEEE Transactions on Circuits and Systems for Video Technology*, vol. 27, no. 3, pp. 540–553, 2016.
- [2] R. Feris, R. Bobbitt, L. Brown, and S. Pankanti, "Attribute-based people search: Lessons learnt from a practical surveillance system," in *Proceedings of International Conference on Multimedia Retrieval*, 2014, p. 153.
- [3] J. Nhan, L. Huey, and R. Broll, "Digilantism: An analysis of crowd-sourcing and the boston marathon bombings," *The British journal of criminology*, vol. 57, no. 2, pp. 341–361, 2017.
- [4] M. Farenzena, L. Bazzani, A. Perina, V. Murino, and M. Cristani, "Person re-identification by symmetry-driven accumulation of local features," in *Proceedings of the IEEE Conference on Computer Vision and Pattern Recognition*, 2010, pp. 2360–2367.
- [5] W.-S. Zheng, S. Gong, and T. Xiang, "Reidentification by relative distance comparison," *IEEE Transactions on Pattern Analysis and Machine Intelligence*, vol. 35, no. 3, pp. 653–668, 2012.
- [6] R. Zhao, W. Ouyang, and X. Wang, "Unsupervised salience learning for person re-identification," in *Proceedings of the IEEE Conference on Computer Vision and Pattern Recognition*, 2013, pp. 3586–3593.
- [7] R. Vezzani, D. Baltieri, and R. Cucchiara, "People reidentification in surveillance and forensics: A survey," *ACM Computing Surveys (CSUR)*, vol. 46, no. 2, p. 29, 2013.
- [8] W. Li, R. Zhao, T. Xiao, and X. Wang, "Deepreid: Deep filter pairing neural network for person re-identification," in *Proceedings of the IEEE Conference on Computer Vision and Pattern Recognition*, 2014, pp. 152–159.
- [9] R. Zhao, W. Ouyang, and X. Wang, "Learning mid-level filters for person re-identification," in *Proceedings of the IEEE Conference on Computer Vision and Pattern Recognition*, 2014, pp. 144–151.
- [10] Y. Yang, J. Yang, J. Yan, S. Liao, D. Yi, and S. Z. Li, "Salient color names for person re-identification," in *Proceedings of the European Conference on Computer Vision*, 2014, pp. 536–551.
- [11] S. Liao, Y. Hu, X. Zhu, and S. Z. Li, "Person re-identification by local maximal occurrence representation and metric learning," in *Proceedings of the IEEE Conference on Computer Vision and Pattern Recognition*, 2015, pp. 2197–2206.
- [12] L. Zheng, Y. Yang, and A. G. Hauptmann, "Person re-identification: Past, present and future," *arXiv preprint arXiv:1610.02984*, 2016.
- [13] Z. Zheng, L. Zheng, and Y. Yang, "Unlabeled samples generated by gan improve the person re-identification baseline in vitro," in *Proceedings of the IEEE International Conference on Computer Vision*, 2017, pp. 3754–3762.
- [14] W. Chen, X. Chen, J. Zhang, and K. Huang, "Beyond triplet loss: a deep quadruplet network for person re-identification," in *Proceedings of the IEEE Conference on Computer Vision and Pattern Recognition*, 2017, pp. 403–412.
- [15] C. Song, Y. Huang, W. Ouyang, and L. Wang, "Mask-guided contrastive attention model for person re-identification," in *Proceedings of the IEEE Conference on Computer Vision and Pattern Recognition*, 2018, pp. 1179–1188.
- [16] S. Bai, P. Tang, P. H. Torr, and L. Jan Latecki, "Re-ranking via metric fusion for object retrieval and person re-identification," in *Proceedings of the IEEE Conference on Computer Vision and Pattern Recognition*, 2019, pp. 740–749.
- [17] Z. Wang, J. Jiang, Y. Yu, and S. Satoh, "Incremental re-identification by cross-direction and cross-ranking adaption," *IEEE Transactions on Multimedia*, 2019.
- [18] W. Li, X. Zhu, and S. Gong, "Harmonious attention network for person re-identification," in *Proceedings of the IEEE Conference on Computer Vision and Pattern Recognition*, 2018, pp. 2285–2294.
- [19] Z. Zhong, L. Zheng, Z. Zheng, S. Li, and Y. Yang, "Camera style adaptation for person re-identification," in *Proceedings of the IEEE Conference on Computer Vision and Pattern Recognition*, 2018, pp. 5157–5166.
- [20] J. Wang, X. Zhu, S. Gong, and W. Li, "Transferable joint attribute-identity deep learning for unsupervised person re-identification," in *Proceedings of the IEEE Conference on Computer Vision and Pattern Recognition*, 2018, pp. 2275–2284.
- [21] L. Zheng, L. Shen, L. Tian, S. Wang, J. Wang, and Q. Tian, "Scalable person re-identification: A benchmark," in *Proceedings of the IEEE International Conference on Computer Vision*, 2015, pp. 1116–1124.
- [22] X. Zhang, H. Luo, X. Fan, W. Xiang, Y. Sun, Q. Xiao, W. Jiang, C. Zhang, and J. Sun, "Alignedreid: Surpassing human-level performance in person re-identification," *arXiv preprint arXiv:1711.08184*, 2017.
- [23] Z. Wu, Y. Li, and R. J. Radke, "Viewpoint invariant human re-identification in camera networks using pose priors and subject-discriminative features," *IEEE Transactions on Pattern Analysis and Machine Intelligence*, vol. 37, no. 5, pp. 1095–1108, 2014.
- [24] C. Su, J. Li, S. Zhang, J. Xing, W. Gao, and Q. Tian, "Pose-driven deep convolutional model for person re-identification," in *Proceedings of the IEEE Conference on Computer Vision and Pattern Recognition*, 2017, pp. 3960–3969.
- [25] X. Qian, Y. Fu, T. Xiang, W. Wang, J. Qiu, Y. Wu, Y.-G. Jiang, and X. Xue, "Pose-normalized image generation for person re-identification," in *Proceedings of the European Conference on Computer Vision*, 2018, pp. 650–667.
- [26] J. Liu, B. Ni, Y. Yan, P. Zhou, S. Cheng, and J. Hu, "Pose transferrable person re-identification," in *Proceedings of the IEEE Conference on Computer Vision and Pattern Recognition*, 2018, pp. 4099–4108.
- [27] L. Zheng, Y. Huang, H. Lu, and Y. Yang, "Pose invariant embedding for deep person re-identification," *IEEE Transactions on Image Processing*, 2019.
- [28] D. Xu, J. Chen, C. Liang, Z. Wang, and R. Hu, "Cross-view identical part area alignment for person re-identification," in *IEEE International Conference on Acoustics, Speech and Signal Processing*, 2019, pp. 2462–2466.
- [29] I. Kviatkovsky, A. Adam, and E. Rivlin, "Color invariants for person reidentification," *IEEE Transactions on Pattern Analysis and Machine Intelligence*, vol. 35, no. 7, pp. 1622–1634, 2012.
- [30] Y. Wang, R. Hu, C. Liang, C. Zhang, and Q. Leng, "Camera compensation using a feature projection matrix for person reidentification," *IEEE Transactions on Circuits and Systems for Video Technology*, vol. 24, no. 8, pp. 1350–1361, 2014.
- [31] F. Ma, X. Zhu, X. Zhang, L. Yang, M. Zuo, and X.-Y. Jing, "Low illumination person re-identification," *Multimedia Tools and Applications*, vol. 78, no. 1, pp. 337–362, 2019.
- [32] Z. Zeng, Z. Wang, Z. Wang, Y.-Y. Chuang, and S. Satoh, "Illumination-adaptive person re-identification," *arXiv preprint arXiv:1905.04525*, 2019.
- [33] W.-S. Zheng, X. Li, T. Xiang, S. Liao, J. Lai, and S. Gong, "Partial person re-identification," in *Proceedings of the IEEE International Conference on Computer Vision*, 2015, pp. 4678–4686.
- [34] J. Zhuo, Z. Chen, J. Lai, and G. Wang, "Occluded person re-identification," in *IEEE International Conference on Multimedia and Expo*, 2018, pp. 1–6.
- [35] L. He, J. Liang, H. Li, and Z. Sun, "Deep spatial feature reconstruction for partial person re-identification: Alignment-free approach," in *Proceedings of the IEEE Conference on Computer Vision and Pattern Recognition*, 2018, pp. 7073–7082.
- [36] A. Bedagkar-Gala and S. K. Shah, "A survey of approaches and trends in person re-identification," *Image and Vision Computing*, vol. 32, no. 4, pp. 270–286, 2014.
- [37] M. Gou, Z. Wu, A. Rates-Borras, O. Camps, R. J. Radke *et al.*, "A systematic evaluation and benchmark for person re-identification: Features, metrics, and datasets," *IEEE Transactions on Pattern Analysis and Machine Intelligence*, vol. 41, no. 3, pp. 523–536, 2018.

- [38] A. Nambiar, A. Bernardino, and J. C. Nascimento, "Gait-based person re-identification: A survey," *ACM Computing Surveys (CSUR)*, vol. 52, no. 2, p. 33, 2019.
- [39] Q. Leng, M. Ye, and Q. Tian, "A survey of open-world person re-identification," *IEEE Transactions on Circuits and Systems for Video Technology*, 2019.
- [40] N. Gheissari, T. B. Sebastian, and R. Hartley, "Person reidentification using spatiotemporal appearance," in *Proceedings of the IEEE Conference on Computer Vision and Pattern Recognition*, 2006, pp. 1528–1535.
- [41] D. Gray and H. Tao, "Viewpoint invariant pedestrian recognition with an ensemble of localized features," in *Proceedings of the European Conference on Computer Vision*, 2008, pp. 262–275.
- [42] Y. Shen, W. Lin, J. Yan, M. Xu, J. Wu, and J. Wang, "Person re-identification with correspondence structure learning," in *Proceedings of the IEEE Conference on Computer Vision and Pattern Recognition*, 2015, pp. 3200–3208.
- [43] C. Su, F. Yang, S. Zhang, Q. Tian, L. S. Davis, and W. Gao, "Multi-task learning with low rank attribute embedding for person re-identification," in *Proceedings of the IEEE International Conference on Computer Vision*, 2015, pp. 3739–3747.
- [44] T. Matsukawa, T. Okabe, E. Suzuki, and Y. Sato, "Hierarchical gaussian descriptor for person re-identification," in *Proceedings of the IEEE Conference on Computer Vision and Pattern Recognition*, 2016, pp. 1363–1372.
- [45] K. Q. Weinberger, J. Blitzer, and L. K. Saul, "Distance metric learning for large margin nearest neighbor classification," in *Proceedings of the Advances in Neural Information Processing Systems*, 2006, pp. 1473–1480.
- [46] J. V. Davis, B. Kulis, P. Jain, S. Sra, and I. S. Dhillon, "Information-theoretic metric learning," in *Proceedings of International Conference on Machine Learning*, 2007, pp. 209–216.
- [47] M. Koestinger, M. Hirzer, P. Wohlhart, P. M. Roth, and H. Bischof, "Large scale metric learning from equivalence constraints," in *Proceedings of the IEEE Conference on Computer Vision and Pattern Recognition*, 2012, pp. 2288–2295.
- [48] M. Hirzer, P. M. Roth, M. Köstinger, and H. Bischof, "Relaxed pairwise learned metric for person re-identification," in *Proceedings of the European Conference on Computer Vision*, 2012, pp. 780–793.
- [49] S. Liao and S. Z. Li, "Efficient psd constrained asymmetric metric learning for person re-identification," in *Proceedings of the IEEE International Conference on Computer Vision*, 2015, pp. 3685–3693.
- [50] A. Mignon and F. Jurie, "Pcca: A new approach for distance learning from sparse pairwise constraints," in *Proceedings of the IEEE Conference on Computer Vision and Pattern Recognition*, 2012, pp. 2666–2672.
- [51] S. Pedagadi, J. Orwell, S. Velastin, and B. Boghossian, "Local fisher discriminant analysis for pedestrian re-identification," in *Proceedings of the IEEE Conference on Computer Vision and Pattern Recognition*, 2013, pp. 3318–3325.
- [52] F. Xiong, M. Gou, O. Camps, and M. Szaier, "Person re-identification using kernel-based metric learning methods," in *Proceedings of the European Conference on Computer Vision*, 2014, pp. 1–16.
- [53] L. Zhang, T. Xiang, and S. Gong, "Learning a discriminative null space for person re-identification," in *Proceedings of the IEEE Conference on Computer Vision and Pattern Recognition*, 2016, pp. 1239–1248.
- [54] E. Ahmed, M. Jones, and T. K. Marks, "An improved deep learning architecture for person re-identification," in *Proceedings of the IEEE Conference on Computer Vision and Pattern Recognition*, 2015, pp. 3908–3916.
- [55] R. R. Varior, B. Shuai, J. Lu, D. Xu, and G. Wang, "A siamese long short-term memory architecture for human re-identification," in *Proceedings of the European Conference on Computer Vision*, 2016, pp. 135–153.
- [56] R. R. Varior, M. Haloi, and G. Wang, "Gated siamese convolutional neural network architecture for human re-identification," in *Proceedings of the European Conference on Computer Vision*, 2016, pp. 791–808.
- [57] D. Cheng, Y. Gong, S. Zhou, J. Wang, and N. Zheng, "Person re-identification by multi-channel parts-based cnn with improved triplet loss function," in *Proceedings of the IEEE Conference on Computer Vision and Pattern Recognition*, 2016, pp. 1335–1344.
- [58] C. Su, S. Zhang, J. Xing, W. Gao, and Q. Tian, "Deep attributes driven multi-camera person re-identification," in *Proceedings of the European Conference on Computer Vision*, 2016, pp. 475–491.
- [59] T. Xiao, H. Li, W. Ouyang, and X. Wang, "Learning deep feature representations with domain guided dropout for person re-identification," in *Proceedings of the IEEE Conference on Computer Vision and Pattern Recognition*, 2016, pp. 1249–1258.
- [60] J. Xu, R. Zhao, F. Zhu, H. Wang, and W. Ouyang, "Attention-aware compositional network for person re-identification," in *Proceedings of the IEEE Conference on Computer Vision and Pattern Recognition*, 2018, pp. 2119–2128.
- [61] X. Chang, T. M. Hospedales, and T. Xiang, "Multi-level factorisation net for person re-identification," in *Proceedings of the IEEE Conference on Computer Vision and Pattern Recognition*, 2018, pp. 2109–2118.
- [62] Z. Zhang, C. Lan, W. Zeng, and Z. Chen, "Densely semantically aligned person re-identification," in *Proceedings of the IEEE Conference on Computer Vision and Pattern Recognition*, 2019, pp. 667–676.
- [63] M. Zheng, S. Karanam, Z. Wu, and R. J. Radke, "Re-identification with consistent attentive siamese networks," in *Proceedings of the IEEE Conference on Computer Vision and Pattern Recognition*, 2019, pp. 5735–5744.
- [64] S. Ouyang, T. Hospedales, Y.-Z. Song, X. Li, C. C. Loy, and X. Wang, "A survey on heterogeneous face recognition: Sketch, infra-red, 3d and low-resolution," *Image and Vision Computing*, vol. 56, pp. 28–48, 2016.
- [65] K. Wang, Q. Yin, W. Wang, S. Wu, and L. Wang, "A comprehensive survey on cross-modal retrieval," *arXiv preprint arXiv:1607.06215*, 2016.
- [66] I. B. Barbosa, M. Cristani, A. Del Bue, L. Bazzani, and V. Murino, "Re-identification with rgb-d sensors," in *Proceedings of the European Conference on Computer Vision*, 2012, pp. 433–442.
- [67] A. Mogelmoose, C. Bahnsen, T. Moeslund, A. Clapes, and S. Escalera, "Tri-modal person re-identification with rgb, depth and thermal features," in *Proceedings of the IEEE Conference on Computer Vision and Pattern Recognition Workshops*, 2013, pp. 301–307.
- [68] M. Munaro, A. Basso, A. Fossati, L. Van Gool, and E. Menegatti, "3d reconstruction of freely moving persons for re-identification with a depth sensor," in *IEEE International Conference on Robotics and Automation*, 2014, pp. 4512–4519.
- [69] A. Haque, A. Alahi, and L. Fei-Fei, "Recurrent attention models for depth-based person identification," in *Proceedings of the IEEE Conference on Computer Vision and Pattern Recognition*, 2016, pp. 1229–1238.
- [70] A. Wu, W.-S. Zheng, and J.-H. Lai, "Robust depth-based person re-identification," *IEEE Transactions on Image Processing*, vol. 26, no. 6, pp. 2588–2603, 2017.
- [71] Z. Wang, Z. Wang, Y. Zheng, Y.-Y. Chuang, and S. Satoh, "Learning to reduce dual-level discrepancy for infrared-visible person re-identification," in *Proceedings of the IEEE Conference on Computer Vision and Pattern Recognition*, 2019.
- [72] J. Jiao, W.-S. Zheng, A. Wu, X. Zhu, and S. Gong, "Deep low-resolution person re-identification," in *Proceedings of the AAAI Conference on Artificial Intelligence*, 2018.
- [73] L. Pang, Y. Wang, Y.-Z. Song, T. Huang, and Y. Tian, "Cross-domain adversarial feature learning for sketch re-identification," in *ACM Multimedia*, 2018.
- [74] S. Li, T. Xiao, H. Li, W. Yang, and X. Wang, "Identity-aware textual-visual matching with latent co-attention," in *Proceedings of the IEEE International Conference on Computer Vision*, 2017.
- [75] A. Wu, W.-S. Zheng, H.-X. Yu, S. Gong, and J. Lai, "Rgb-infrared cross-modality person re-identification," in *Proceedings of the IEEE International Conference on Computer Vision*, 2017, pp. 5380–5389.
- [76] S. Li, T. Xiao, H. Li, B. Zhou, D. Yue, and X. Wang, "Person search with natural language description," in *Proceedings of the IEEE Conference on Computer Vision and Pattern Recognition*, 2017.
- [77] D. Gray, S. Brennan, and H. Tao, "Evaluating appearance models for recognition, reacquisition, and tracking," in *Proc. IEEE International Workshop on Performance Evaluation for Tracking and Surveillance (PETS)*, vol. 3, no. 5, 2007, pp. 1–7.
- [78] D. Baltieri, R. Vezzani, and R. Cucchiara, "3dpes: 3d people dataset for surveillance and forensics," in *Proceedings of the joint ACM workshop on Human gesture and behavior understanding*, 2011, pp. 59–64.
- [79] W.-S. Zheng, T. Xiang, and S. Gong, "Associating groups of people," in *British Machine Vision Conference*, 2011.
- [80] M. Hirzer, C. Beleznai, P. M. Roth, and H. Bischof, "Person re-identification by descriptive and discriminative classification," in *Scandinavian conference on Image analysis*, 2011, pp. 91–102.
- [81] P. M. Roth, M. Hirzer, M. Köstinger, C. Beleznai, and H. Bischof, "Mahalanobis Distance Learning for Person Re-Identification," in *Person Re-Identification*, ser. Advances in Computer Vision and Pattern Recognition, 2014, pp. 247–267.

- [82] D. S. Cheng, M. Cristani, M. Stoppa, L. Bazzani, and V. Murino, "Custom pictorial structures for re-identification," in *British Machine Vision Conference*, 2011.
- [83] X. Li, W.-S. Zheng, X. Wang, T. Xiang, and S. Gong, "Multi-scale learning for low-resolution person re-identification," in *Proceedings of the IEEE International Conference on Computer Vision*, 2015, pp. 3765–3773.
- [84] X.-Y. Jing, X. Zhu, F. Wu, X. You, Q. Liu, D. Yue, R. Hu, and B. Xu, "Super-resolution person re-identification with semi-coupled low-rank discriminant dictionary learning," in *Proceedings of the IEEE Conference on Computer Vision and Pattern Recognition*, 2015, pp. 695–704.
- [85] Z. Wang, R. Hu, Y. Yu, J. Jiang, C. Liang, and J. Wang, "Scale-adaptive low-resolution person re-identification via learning a discriminating surface," in *Proceedings of the International Joint Conferences on Artificial Intelligence*, 2016, pp. 2669–2675.
- [86] D. Nguyen, H. Hong, K. Kim, and K. Park, "Person recognition system based on a combination of body images from visible light and thermal cameras," *Sensors*, vol. 17, no. 3, p. 605, 2017.
- [87] Y.-C. Chen, W.-S. Zheng, J.-H. Lai, and P. C. Yuen, "An asymmetric distance model for cross-view feature mapping in person reidentification," *IEEE Transactions on Circuits and Systems for Video Technology*, vol. 27, no. 8, pp. 1661–1675, 2016.
- [88] X. Wang, G. Doretto, T. Sebastian, J. Rittscher, and P. Tu, "Shape and appearance context modeling," in *Proceedings of the IEEE International Conference on Computer Vision*, 2007, pp. 1–8.
- [89] K. Li, Z. Ding, S. Li, and Y. Fu, "Discriminative semi-coupled projective dictionary learning for low-resolution person re-identification," in *Proceedings of the AAAI Conference on Artificial Intelligence*, 2018.
- [90] Z. Wang, M. Ye, F. Yang, X. Bai, and S. Satoh, "Cascaded sr-gan for scale-adaptive low resolution person re-identification," in *Proceedings of the International Joint Conferences on Artificial Intelligence*, 2018, pp. 3891–3897.
- [91] Y.-C. Chen, Y.-J. Li, X. Du, and Y.-C. F. Wang, "Learning resolution-invariant deep representations for person re-identification," in *Proceedings of the AAAI Conference on Artificial Intelligence*, 2019.
- [92] S. Mao, S. Zhang, and M. Yang, "Resolution-invariant person re-identification," in *Proceedings of the International Joint Conferences on Artificial Intelligence*, 2019.
- [93] M. Ye, X. Lan, J. Li, and P. C. Yuen, "Hierarchical discriminative learning for visible thermal person re-identification," in *Proceedings of the AAAI Conference on Artificial Intelligence*, 2018.
- [94] M. Ye, Z. Wang, X. Lan, and P. C. Yuen, "Visible thermal person re-identification via dual-constrained top-ranking," in *Proceedings of the International Joint Conferences on Artificial Intelligence*, 2018, pp. 1092–1099.
- [95] P. Dai, R. Ji, H. Wang, Q. Wu, and Y. Huang, "Cross-modality person re-identification with generative adversarial training," in *Proceedings of the International Joint Conferences on Artificial Intelligence*, 2018, pp. 677–683.
- [96] D. Chen, H. Li, X. Liu, Y. Shen, J. Shao, Z. Yuan, and X. Wang, "Improving deep visual representation for person re-identification by global and local image-language association," in *Proceedings of the European Conference on Computer Vision*, 2018, pp. 54–70.
- [97] F. Ma, X.-Y. Jing, Y. Yao, X. Zhu, and Z. Peng, "High-resolution and low-resolution video person re-identification: A benchmark," *IEEE Access*, vol. 7, pp. 63 426–63 436, 2019.
- [98] J. K. Kang, T. M. Hoang, and K. R. Park, "Person re-identification between visible and thermal camera images based on deep residual cnn using single input," *IEEE Access*, vol. 7, pp. 57 972–57 984, 2019.
- [99] M. Ye, C. Liang, Z. Wang, Q. Leng, J. Chen, and J. Liu, "Specific person retrieval via incomplete text description," in *Proceedings of International Conference on Multimedia Retrieval*, 2015, pp. 547–550.
- [100] Z. Wang, R. Hu, Y. Yu, C. Liang, and W. Huang, "Multi-level fusion for person re-identification with incomplete marks," in *ACM Multimedia*, 2015.
- [101] Z. Yin, W.-S. Zheng, A. Wu, H.-X. Yu, H. Wan, X. Guo, F. Huang, and J. Lai, "Adversarial attribute-image person re-identification," in *Proceedings of the International Joint Conferences on Artificial Intelligence*, 2018, pp. 1100–1106.
- [102] T. Chen, C. Xu, and J. Luo, "Improving text-based person search by spatial matching and adaptive threshold," in *IEEE Winter Conference on Applications of Computer Vision*, 2018, pp. 1879–1887.